Tumor Necrosis Factor-α Blocks Differentiation and Enhances Suppressive Activity of Immature Myeloid Cells during Chronic Inflammation

Moshe Sade-Feldman,[1] Julia Kanterman,[1] Eliran Ish-Shalom,[1] Mazal Elnekave,[2] Elad Horwitz,[1] and Michal Baniyash[1,*]
[1]The Lautenberg Center for General and Tumor Immunology, The Institute for Medical Research Israel-Canada
[2]Institute of Dental Sciences, School of Dental Medicine
The Hebrew University Hadassah Medical School, Jerusalem 91120, Israel
*Correspondence: baniyash@cc.huji.ac.il
http://dx.doi.org/10.1016/j.immuni.2013.02.007

SUMMARY

Elevated concentrations of tumor necrosis factor-α (TNF-α) are detected in pathologies characterized by chronic inflammation. Whether TNF-α plays a role in manipulating the host's immune system toward generating an immunosuppressive milieu, typical of ongoing chronic inflammation, is unclear. Here we showed that TNF-α exhibited a dual function during chronic inflammation: arresting differentiation of immature myeloid-derived suppressor cells (MDSCs) primarily via the S100A8 and S100A9 inflammatory proteins and their corresponding receptor (RAGE) and augmenting MDSC suppressive activity. These functions led to in vivo T and NK cell dysfunction accompanied by T cell antigen receptor ζ chain downregulation. Furthermore, administration of etanercept (TNF-α antagonist) during early chronic inflammatory stages reduced MDSCs' suppressive activity and enhanced their maturation into dendritic cells and macrophages, resulting in the restoration of in vivo immune functions and recovery of ζ chain expression. Thus, TNF has a fundamental role in promoting an immunosuppressive environment generated during chronic inflammation.

INTRODUCTION

Numerous pathologies, including cancer, infectious diseases, and autoimmune disorders, are characterized by chronic inflammation and an immunosuppressive environment, which leads to T and natural killer (NK) cell dysfunction associated with T cell receptor (TCR) ζ chain (CD247) downregulation. ζ chain is a key component responsible for the initiation of immune responses mediated by these two cell types and is affected by the generated immunosuppressive milieu (Baniyash, 2004, 2006). Various studies, including our own, have shown that chronic inflammation-dependent immunosuppression is mediated by myeloid-derived suppressor cells (MDSCs), which represent a heterogeneous immature cell population of the myeloid lineage (Ezernitchi et al., 2006; Vaknin et al., 2008). Expansion of MDSCs coexpressing Gr1$^+$CD11b$^+$ in mice and CD11b$^+$CD14$^-$CD33$^+$, LIN$^-$HLA-DR$^-$CD33$^+$, or CD14$^+$CD11b$^+$ in humans is observed in some of the above-mentioned pathologies, resulting in suppression of immune responses (Gabrilovich and Nagaraj, 2009; Ostrand-Rosenberg and Sinha, 2009; Serafini et al., 2006).

Chronic inflammation is mediated by a complex network of proinflammatory cytokines (IFN-γ, IL-1β, IL-6), chemokines (CXCL5, CCL2), and growth factors (GM-CSF, VEGF) persistently secreted by normal self or modified cells including tumor cells, thus affecting MDSC accumulation, activation, and suppressive function (Bunt et al., 2006, 2007; Gallina et al., 2006; Huang et al., 2007; Kusmartsev et al., 2008; Serafini et al., 2004; Song et al., 2005; Yang et al., 2008). We previously showed that elevated serum concentrations of the proinflammatory cytokines IFN-γ and TNF-α detected in chronically inflamed mice correlate with extensive recruitment and expansion of MDSCs (Vaknin et al., 2008). Although our studies indicated that IFN-γ plays a role in the initial stage of the developing inflammation (Bronstein-Sitton et al., 2003), affecting generation and recruitment of MDSCs, the role of TNF-α in MDSC-dependent immunosuppression is, as yet, unknown.

TNF-α is a proinflammatory, multifunctional, and immunomodulating cytokine (Pfeffer, 2003) that has been shown to be harmful in various chronic pathologies such as rheumatoid arthritis, psoriasis, type II diabetes, Crohn's disease, and cancer (Balkwill, 2006; Feldmann, 2002; Kopf et al., 2010; Reich et al., 2005). Therefore, several FDA-approved TNF-α antagonists are currently in clinical use for such pathologies (Cheng et al., 2008). One of these antagonists, etanercept, a soluble form of the TNF receptor (Goffe and Cather, 2003), has been shown to be effective in treating patients with rheumatoid arthritis and cancer (Friedberg et al., 2008; Scott, 2005; Wilson, 2008). However, the mechanism by which TNF-α and accordingly its antagonists regulate the host's immune system during chronic inflammation remains unclear. Our observations demonstrating elevated amounts of TNF-α and MDSCs in chronically inflamed mice in conjunction with the TNF-α characteristics led us to suggest that TNF-α could play an important role in inducing the immunosuppressive environment through MDSCs.

To test our hypothesis, we applied our previously described in vivo mouse model system for chronic inflammation (Bronstein-Sitton et al., 2003; Vaknin et al., 2008) on *Tnf*$^{-/-}$ and *Tnf*$^{+/+}$ (wild-type) mice and compared their immune competence under the generated inflammatory conditions. Herein we demonstrate that during chronic inflammation, TNF-α plays a key role in manipulating the suppressive environment by controlling MDSC

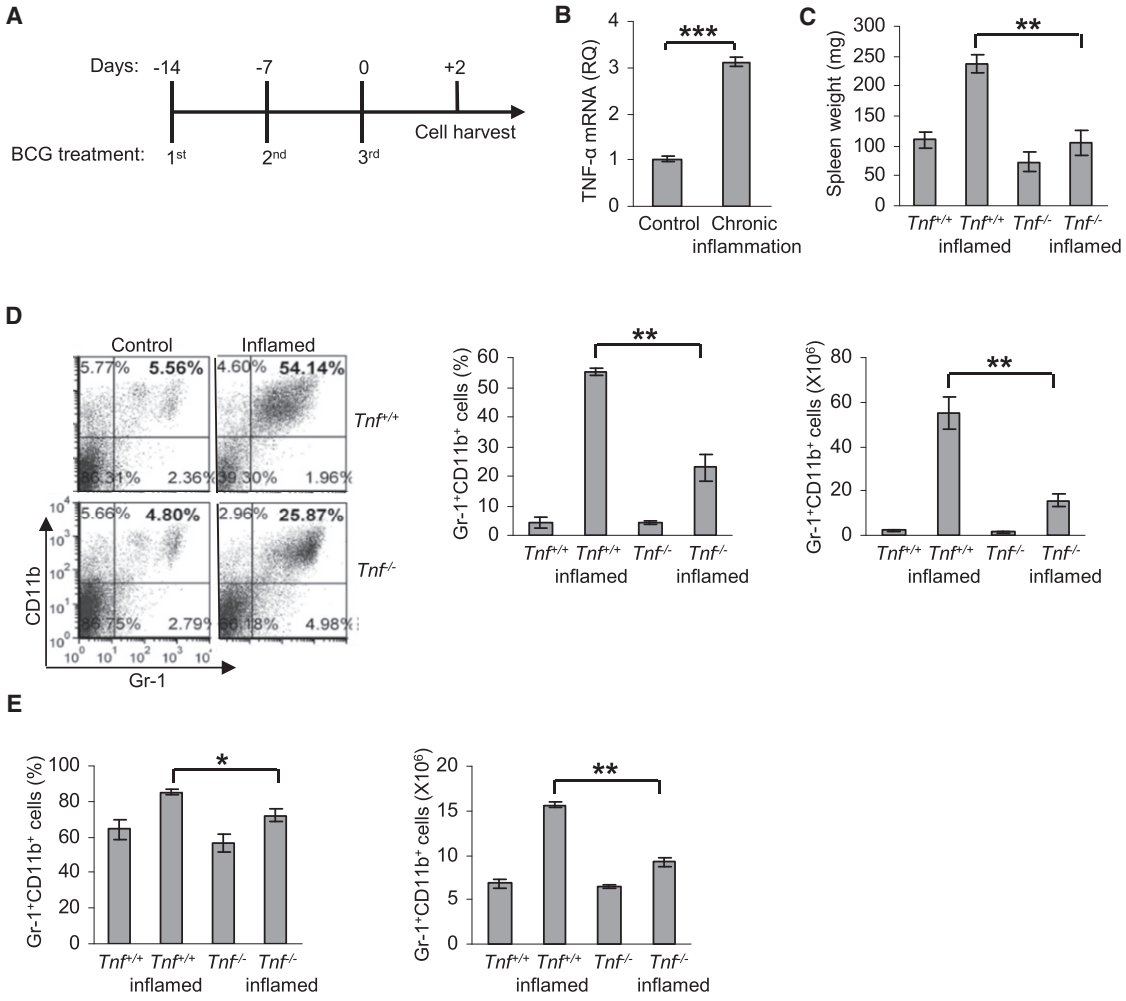

Figure 1. TNF-α Augments the Chronic Inflammatory Response

(A) A mouse model for chronic inflammation was established by repeated injections of heat-killed BCG bacteria; the mice were sacrificed at day +2, after the last treatment.

(B) Quantitative PCR analysis for TNF-α mRNA expression in isolated MDSCs from control (noninflamed) and chronically inflamed *Tnf*$^{+/+}$ mice, presented as relative quantification (RQ) compared to the expression in MDSCs from control mice, set as 1. Data of three experiments are presented (mean ± SEM, n = 3 per group).

(C) The weight of spleens was evaluated at day +2 after the third BCG injection.

(D and E) The percentage and absolute numbers of MDSCs (Gr-1$^+$CD11b$^+$) at day +2 after the last BCG treatment in the spleen (D) and bone marrow (BM) (E) are presented. Results are representative of three or more independent experiments (error bars show SD, n = 4–7 per group).

*$p < 0.03$; **$p < 0.005$; ***$p < 0.0001$ (t test). See also Figure S1.

features: arresting their maturation via the S100A8 and S100A9 proinflammatory proteins and their corresponding receptor, RAGE, and enhancing intrinsic MDSC suppressive function by increasing activity of both inducible nitric oxide synthase (iNOS) and arginase 1, resulting in the elevation of reactive oxygen species (ROS) production and NO^-. These lead to T and NK cell in vivo dyfunctions associated with ζ chain downregulation, a phenomenon that is reversible upon MDSC depletion. Finally, treatment of mice during early stages of chronic inflammation with etanercept leads to an increased maturation of MDSCs into mature myeloid cells (dendritic cells and macrophages) and reduction in their immunosuppressive activity, as reflected by a retrieval of in vivo T and NK cell effector immune functions and a recovery of ζ chain expression. Our results demonstrate a critical role of TNF-α in promoting a suppressive milieu during chronic inflammation and highlight the underlying mechanisms.

RESULTS

TNF-α Is Involved in Enhanced MDSC Accumulation Observed during Chronic Inflammation

Sustained exposure of mice to heat-killed pathogens or a single Toll-like receptor (TLR) ligand leads to chronic inflammation as reflected by accumulation of MDSCs and increased serum amounts of IFN-γ and TNF-α, as previously showed by us (Ezernitchi et al., 2006; Vaknin et al., 2008). In addition, our initial analyses depict that MDSCs isolated from chronically inflamed mice (Figure 1A) display elevated TNF-α mRNA amounts (Figure 1B).

These results in conjunction with previous data showing MDSCs' major role in generating an immunosuppressive environment in pathologies characterized by chronic inflammation (Gabrilovich and Nagaraj, 2009; Kanterman et al., 2012; Ostrand-Rosenberg and Sinha, 2009; Serafini et al., 2006) led us to hypothesize that TNF-α under such conditions might affect MDSC accumulation. To test this hypothesis, we first compared the response of *Tnf*$^{+/+}$ and *Tnf*$^{-/-}$ mice to a developing chronic inflammation, induced by repeated heat-killed BCG injections (Figure 1A). The initial results revealed that *Tnf*$^{+/+}$ mice display a greater inflammatory response, indicated by increased spleen weight (Figure 1C) and size (data not shown) when compared to the *Tnf*$^{-/-}$ mice. Moreover, MDSC numbers in the spleen (Figure 1D) and bone marrow (BM) (Figure 1E) of inflamed *Tnf*$^{+/+}$ mice were significantly elevated compared to those of inflamed *Tnf*$^{-/-}$ mice. To rule out the possibility that the decreased accumulation of MDSCs observed in the *Tnf*$^{-/-}$ mice was due to a general reduced expression of proinflammatory cytokines such as IFN-γ, IL-1, and IL-6, previously shown to be involved in MDSC accumulation (Bunt et al., 2006; Gallina et al., 2006; Song et al., 2005), we assessed their expression in the spleen of inflamed *Tnf*$^{+/+}$ and *Tnf*$^{-/-}$ mice. Interestingly, in the absence of TNF-α, the expression of IFN-γ, IL-1, IL-6, and IL-12 were rather upregulated (Figure S1A available online). However, the proinflammatory conditions generated in the absence of TNF-α could not support MDSC accumulation, suggesting a unique role for TNF-α. Further analysis of both inflamed *Tnf*$^{+/+}$ and *Tnf*$^{-/-}$ mice revealed that MDSC distribution surrounding the spleen T cell zones was not affected (Figure S1B) and that TNF-α had no effect on the frequency of the two major MDSC subsets, the granulocytic (CD11b^{+}Ly6G^{+}Ly6C^{lo}) and monocytic (CD11b^{+}Ly6G^{-}Ly6C^{hi}) subpopulations, both in the spleen and bone marrow (BM) (Figure S1C), suggesting that TNF-α targets the whole MDSC population. It is important to note that in all cases we excluded the possibility of neutrophil (CD11b^{+}Ly6G^{+}) presence within the MDSC population, because MDSCs were always positive for the Ly6C marker, and cells expressing only the CD11b^{+}Ly6G^{+} neutrophils markers were not detected (data not shown).

Further analyses revealed that percentages of regulatory T cells (Treg cells; CD4^{+}Foxp3^{+}), reported as immunosuppressive in various chronic pathologies (Vignali et al., 2008), were not affected by TNF-α in the spleen and blood of inflamed *Tnf*$^{-/-}$ versus *Tnf*$^{+/+}$ mice (Figure S1D).

TNF-α Negatively Affects T and NK Cell Functions through MDSC Regulation

The observed reduced MDSC numbers in inflamed *Tnf*$^{-/-}$ mice suggests an improved immunological status. We therefore assessed T and NK cell functions as well as ζ chain expression in inflamed *Tnf*$^{+/+}$ and *Tnf*$^{-/-}$ mice. The results revealed that whereas inflamed *Tnf*$^{+/+}$ mice display a significantly reduced ζ chain expression within T cells, inflamed *Tnf*$^{-/-}$ mice show elevated ζ chain expression (Figure 2A). In contrast, total amount of CD3ε (Figure 2B) and the remaining TCR subunits (data not shown) were similar in all experimental groups, indicating that ζ chain is the sole TCR subunit affected by the developing chronic inflammatory environment. Next we evaluated the in vivo impact of MDSCs on ζ chain expression in T cells. We hypothesized that MDSC depletion could restore ζ chain expression in endogenous (host) immune cells as well as in newly administered (donor) cells, mimicking adoptively transferred assays used today in different immunotherapeutic regimens for various pathologies (Huye and Dotti, 2010; Sutlu and Alici, 2009). Indeed, in vivo depletion of MDSCs in inflamed *Tnf*$^{+/+}$ mice (Figure S2) completely restored ζ chain expression within the host T cells as well as in the adoptively transferred CFSE-labeled T cells (Figure 2C), providing direct evidence of the in vivo effect of MDSCs on ζ chain expression in T cells.

We next tested how lack of TNF-α affects T cell function during developing chronic inflammation. We first compared the ex vivo proliferation of splenic T cells from inflamed *Tnf*$^{+/+}$ mice to those of *Tnf*$^{-/-}$ mice in response to TCR-mediated activation. Although T cells from inflamed *Tnf*$^{+/+}$ mice displayed an impaired proliferative ability, T cells from inflamed *Tnf*$^{-/-}$ mice were only slightly affected (Figure 2D). Subsequently, we tested the ability of T cells to proliferate in vivo in an antigen-specific manner. To this end, mice were first immunized with a plasmid containing cytomegaolovirus promoter, which ectopically expresses the gene for ovalbumin (CMV-OVA). The mice were then subjected to the treatment that induces chronic inflammation. At the peak of the inflammatory response, evaluated by the high numbers of MDSCs, mice were injected intravenously (i.v.) with CFSE-labeled OT-I splenocytes (Figure 2E). Four days later the in vivo proliferative response of CD8^{+} OT-I cells from the spleen of immunized and nonimmunized mice was analyzed. As seen in Figure 2F, only the CD8^{+} OT-I cells in the inflamed *Tnf*$^{-/-}$ group displayed a high proliferative response, and no proliferation was detected in the cells from the inflamed *Tnf*$^{+/+}$ mice. Moreover, we show evidence that the impaired proliferative response observed in the spleen of *Tnf*$^{+/+}$ inflamed mice was MDSC mediated, because in vivo depletion of MDSCs completely restored the ability of CD8^{+} OT-I cells to proliferate, in a similar manner as detected in the noninflamed *Tnf*$^{+/+}$ and *Tnf*$^{-/-}$ immunized mice (Figure 2F).

We next tested how absence of TNF-α affected NK cell functions. First, ζ chain expression was analyzed in NK (NCR1^{+}) cells, because of its role in cell-mediated killing activity associated with activating receptors such as NCR1 (Mao et al., 2010). Although ζ chain expression was reduced in NK cells from inflamed *Tnf*$^{+/+}$ mice, its expression was hardly affected in inflamed *Tnf*$^{-/-}$ mice and was similar to that of the untreated (control) mice of both groups (Figure 3A). In contrast, expression of NCR1 (Figure 3B) was similar in all experimental groups, indicating again that ζ chain is the sole subunit affected by the developing inflammatory environment. Moreover, we also found that the negative effect of TNF-α on ζ chain expression in both host and adoptively transferred CFSE-labeled NK cells during chronic inflammation was MDSC mediated, as shown by the fact that in vivo depletion of MDSCs in inflamed *Tnf*$^{+/+}$ mice completely restored ζ chain expression in NK cells (Figure 3C).

To evaluate how the absence of TNF-α affected in vivo NK cell cytotoxic function during chronic inflammation, we followed their ability to clear allogeneic cells, as previously described (Oberg et al., 2004; Vaknin et al., 2008). Mice were injected i.v. with a mixture of labeled syngeneic (CFSE^{hi}) and allogeneic (CFSE^{lo}) cells, and after 24 hr the percentage of specific allogeneic cell clearance was evaluated (Figure 3D). To exclude the contribution of other cells in the removal of allogeneic CFSE-labeled cells, we

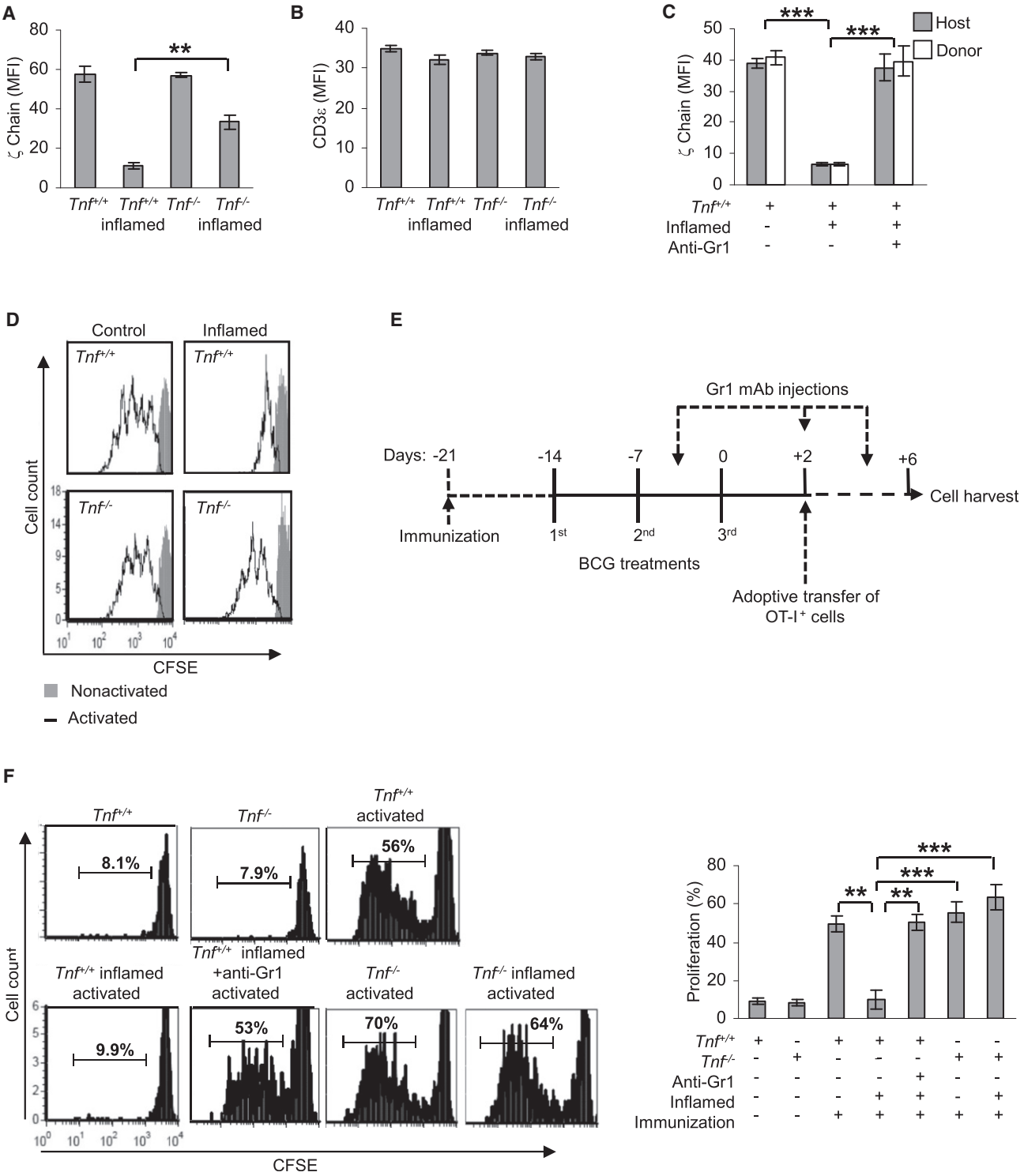

Figure 2. TNF-α Promotes T Cell Dysfunction via MDSCs

(A and B) Splenic CD3$^+$ cells were fixed, permeabilized, and double stained for total expression of the ζ (A) or CD3ε (B) chains, as shown by mean fluorescence intensity (MFI). ζ chain expression plots are of gated CD3$^+$ cells.

(C) MDSCs were in vivo depleted in inflamed *Tnf*$^{+/+}$ mice by three i.p. injections of Gr1 mAbs. 12 hr later, CFSE-labeled splenocytes from normal *Tnf*$^{+/+}$ mice (donor cells) were adoptively transferred into inflamed Gr1 mAb-treated and -untreated mice (hosts). After 24 hr, splenocytes were harvested and stained for ζ expression (MFI) in CD3$^+$ T cells within the CFSE$^+$ (donor) or CFSE$^-$ (host) cells.

(D) Splenocytes were labeled with CFSE and activated with CD3 and CD28 antibodies (black lines), or left nonactivated (gray histograms). The proliferative response was assessed by monitoring cell divisions of gated CFSE-labeled Thy1.2$^+$ cells.

(legend continued on next page)

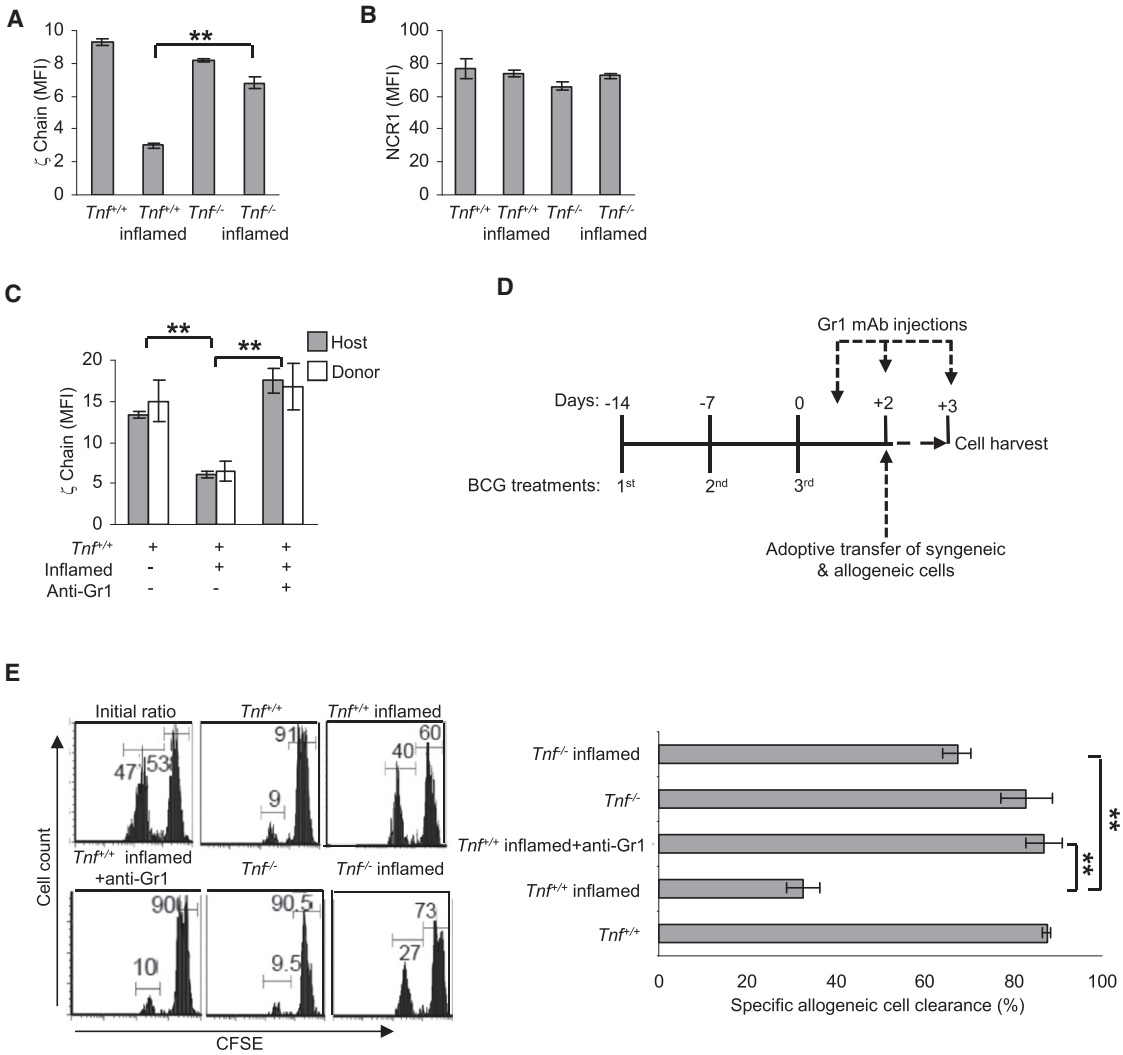

Figure 3. TNF-α Promotes NK Cell Dysfunction via MDSCs

(A and B) MFI of total ζ chain (A) and NCR1 (B) expression in NK (NCR1$^+$) cells.

(C) ζ expression (MFI) was evaluated in NCR1$^+$ NK cells CFSE$^+$ (donor) or CFSE$^-$ (host) cells, after MDSCs were in vivo depleted, as described in Figure 2C.

(D) CFSE-labeled allogeneic (CFSE^{lo}) and syngeneic (CFSE^{hi}) cells were i.v. injected into mice 2 days after the last BCG injection. The cytotoxic activity of NK cells was assessed 24 hr after administration of cells. Additionally, one group was depleted from MDSCs by Gr-1 mAbs.

(E) A representative plot of CFSE allogeneic and syngeneic cell clearance within the spleens of mice is shown (top); numbers indicate the percentages of specific allogeneic cell clearance (bottom).

Results are representative of three or more independent experiments (error bars show SD, n = 4–6 per group). *p < 0.005 (t test). See also Figure S3.

depleted NK cells in vivo, which resulted in almost a complete retention of the allogeneic cells (data not shown). A significantly impaired NK cell function in the spleen (Figure 3E) and blood (Figure S3) of inflamed *Tnf*$^{+/+}$ mice was observed, whereas NK cell function in the inflamed *Tnf*$^{-/-}$ mice was only slightly affected. We also saw that impaired NK cell function in inflamed *Tnf*$^{+/+}$ mice is MDSC mediated, because in vivo depletion of MDSCs completely restored NK cell cytotoxic function (Figures 3E and S3).

TNF-α Blocks MDSC Differentiation into Mature Myeloid Cells

MDSCs are composed of a suppressive heterogeneous immature myeloid cell population that could differentiate into dendritic

(E) Mice were immunized with CMV-OVA plasmid and on day +2 after the last BCG injection the mice were adoptively transferred with 4 × 10^6 CFSE-labeled OT-I splenocytes into inflamed or noninflamed mice. Additionally, one group was treated for the depletion of MDSCs by Gr-1 mAbs. 4 days later, the spleens were harvested to analyze the proliferation of the transferred OT-I CD8$^+$ T cells by flow cytometry.

(F) A representative plot gated on dividing OT-I CD8$^+$ T cells in the spleens of inflamed and noninflamed mice (top); numbers indicate the percentage of dividing cells (bottom).

Results are representative of three independent experiments (error bars show SD, n = 4–7 per group). **p < 0.005; ***p < 0.0001 (t test). See also Figure S2.

cells (DCs) ($CD11b^+CD11c^+$) and macrophages ($CD11b^+F4/80^+$) upon an appropriate stimulation (Gabrilovich and Nagaraj, 2009). Based on these data and on our results showing decreased numbers of MDSCs in the spleens of inflamed *Tnf*$^{-/-}$ mice (Figure 1D), we next checked whether mature myeloid cells such as DCs and/or macrophages compensate for the reduced MDSC numbers observed in the inflamed *Tnf*$^{-/-}$ mice. Indeed, high numbers of $CD11c^+$ and $F4/80^+$ cells were observed in the spleens of inflamed *Tnf*$^{-/-}$ mice, relative to those of inflamed *Tnf*$^{+/+}$ mice (Figure 4A). We also observed that the percentage of MHC-II^+CD80^+ double-positive DCs and macrophages significantly increased in inflamed *Tnf*$^{-/-}$ mice, as compared to those in the inflamed *Tnf*$^{+/+}$ mice (Figure 4B), reflecting their increased maturation stage toward antigen-presenting cells (APCs).

We next assessed whether the MDSC-intrinsic TNF-α expression directly affected their differentiation potential. To this end, splenic MDSCs ($CD11b^+Gr\text{-}1^+$ cells) from inflamed *Tnf*$^{+/+}$ and *Tnf*$^{-/-}$ mice (Figure S4A) were incubated with GM-CSF for 3 or 5 days and analyzed for cell phenotype changes. On day 0, immediately after MDSC isolation, the percentages of $CD11c^+$ and $F4/80^+$ cells were similar between the *Tnf*$^{+/+}$ and *Tnf*$^{-/-}$ MDSCs. However, on days +3 and +5, *Tnf*$^{-/-}$ MDSCs displayed a significantly greater differentiation capacity into $CD11c^+$ and $F4/80^+$ cells as compared to *Tnf*$^{+/+}$ MDSCs (Figure 4C). Moreover, the percentage of MHC-II^+CD80^+ double-positive DCs and macrophages derived from the differentiated *Tnf*$^{-/-}$ was significantly increased as compared to those originating in the *Tnf*$^{+/+}$ mice (Figure 4D). Additionally, we also observed that *Tnf*$^{+/+}$ (Figure 4E) and *Tnf*$^{-/-}$ (Figure S4B) MDSCs lost their suppressive activity upon differentiation as reflected by their inability to induce ζ chain downregulation when coincubated with normal T cells as compared to nondifferentiated MDSCs.

Because previous studies have suggested that the S100A8 and S100A9 proinflammatory proteins are directly involved in inhibiting MDSC maturation through the NF-κB signaling pathway (Cheng et al., 2008; Gebhardt et al., 2006; Sinha et al., 2008), we tested the differences in S100A8 and S100A9 mRNA expression between spleens of inflamed *Tnf*$^{+/+}$ and *Tnf*$^{-/-}$ mice. Splenocytes derived from inflamed *Tnf*$^{-/-}$ mice expressed significantly reduced S100A8 and S100A9 mRNA amounts relative to those expressed in cells from inflamed *Tnf*$^{+/+}$ mice (Figure 5A). Moreover, we also observed that freshly isolated MDSCs from inflamed *Tnf*$^{-/-}$ mice had reduced endogenous S100A8 and S100A9 mRNA (Figure 5B) and protein (Figures 5C and S5A) expression relative to those that were detected in MDSCs from inflamed *Tnf*$^{+/+}$ mice. In addition, we also found that MDSCs driven from inflamed *Tnf*$^{-/-}$ mice expressed reduced protein amounts of the RAGE receptor, which is the corresponding receptor for the S100A8 and S100A9 proinflammatory proteins (Figures 5C and S5A).

Finally, we assessed whether exogenous TNF-α could reverse the increased maturation capacity of MDSCs isolated from inflamed *Tnf*$^{-/-}$ mice and whether its effect was mediated via changes in the expression of the S100A8 and S100A9 proteins and RAGE. To this end, MDSCs isolated from inflamed *Tnf*$^{-/-}$ mice were incubated with GM-CSF in the presence or absence of TNF-α for 3 days. On day +3, MDSCs incubated in the presence of TNF-α showed an increased protein expression of both S100A8 and S100A9 and RAGE, as compared to MDSCs incubated in the absence of TNF-α (Figures 5D and S5B). Based on our hypothesis that S100A8 and S100A9 and RAGE blockade could abolish the negative effect of TNF-α, we next evaluated the maturation state of MDSCs on day +5, upon incubation with GM-CSF in the presence or absence of TNF-α and RAGE- or S100A8- and S100A9-neutralizing antibodies applied together or separately. On day +5, MDSCs incubated with TNF-α show significantly reduced maturation compared with that observed in MDSCs incubated with GM-CSF only. Furthermore, we observed that incubation with both RAGE-, S100A8-, and S100A9-neutralizing antibodies fully restored the maturation of MDSCs treated with TNF-α, as compared to MDSCs incubated only with GM-CSF (Figure 5E). We also observed that administration of both RAGE-, S100A8-, and S100A9-neutralizing antibodies significantly increased the maturation capacity of MDSCs treated only with GM-CSF, reaching almost 100%. Similar results were detected in MDSCs from inflamed *Tnf*$^{+/+}$ mice (Figure S5C), underlying the impact of exogenous TNF-α on the maturation capacity of MDSCs mediated through S100A8 and S100A9 and RAGE.

TNF-α Enhances MDSC Suppressive Activity

To test the immunosuppressive function of MDSCs, we coincubated MDSCs isolated from the spleens of inflamed *Tnf*$^{+/+}$ and *Tnf*$^{-/-}$ mice at different ratios in relation to isolated T cells. We observed that *Tnf*$^{-/-}$ MDSCs displayed poor immunosuppressive activity relative to *Tnf*$^{+/+}$ MDSCs, as reflected by the induction of a milder ζ chain downregulation (Figure 6A) and a reduced suppressive effect on T cell proliferation (Figures 6B and S6A), suggesting that TNF-α affects not only MDSC differentiation but also their state of activation.

It was previously demonstrated that TNF-α regulates the activity of both iNOS and arginase 1 enzymes in endothelial and malignant cell lines (Binder et al., 1999; Gao et al., 2007). Because these enzymes are known to be involved in MDSC suppressive activity, through the production of NO^- and ROS and arginine deprivation (Bronte and Zanovello, 2005; Rodríguez and Ochoa, 2008), we evaluated their expression and activity in MDSCs isolated from inflamed *Tnf*$^{+/+}$ and *Tnf*$^{-/-}$ mice. A significantly reduced iNOS mRNA (Figure 6C) and protein (Figure 6D) expression were observed in *Tnf*$^{-/-}$ MDSCs as compared to that seen in *Tnf*$^{+/+}$ MDSCs. In contrast, no significant differences were observed between the groups in arginase 1 expression (Figures 6C and 6D). However, evaluation of ROS production (Figure 6E) and both iNOS (Figure 6F) and arginase 1 (Figure 6G) activities revealed that the enzymes' activity was significantly reduced in inflamed *Tnf*$^{-/-}$ MDSCs compared to that seen in *Tnf*$^{+/+}$ MDSCs. Similar results were observed in vivo when analyzing peripheral blood of inflamed *Tnf*$^{+/+}$ and *Tnf*$^{-/-}$ mice. In this case, both inflamed *Tnf*$^{+/+}$ and *Tnf*$^{-/-}$ mice had similar percentages of MDSCs (Figure S6B). However, in the inflamed *Tnf*$^{-/-}$ mice, the negative effect on ζ chain expression was negligible as compared to that observed in the inflamed *Tnf*$^{+/+}$ mice (Figure S6C). Further analysis of the peripheral blood MDSCs revealed that the suppressive activity of MDSCs from *Tnf*$^{-/-}$ mice was significantly reduced as compared to that observed in *Tnf*$^{+/+}$ mice, by showing reduced ability to produce NO^- (Figure S6D) and ROS

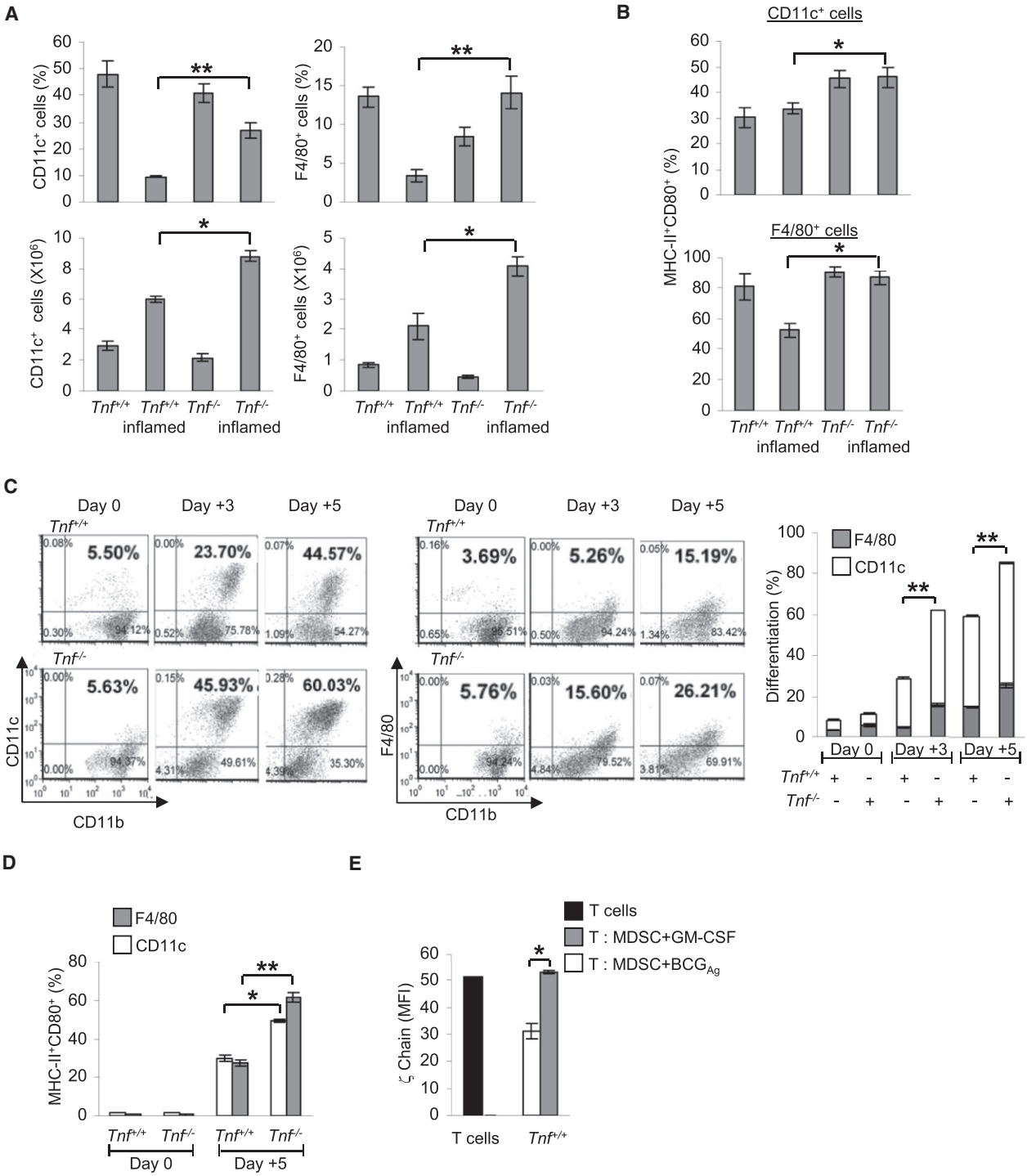

Figure 4. TNF-α Induces Arrest in MDSC Differentiation

(A) A profile of the percentage and absolute number of splenic CD11c$^+$ and F4/80$^+$ cells, gated on CD11b$^+$ cells, in the spleen is presented.

(B) The expression of MHCII$^+$CD80$^+$ in CD11c$^+$ and F4/80$^+$ spleen-derived cells.

(C) MDSCs isolated from spleens of inflamed mice were cultured with GM-CSF for 3 and 5 days, and the cells' phenotype was evaluated. Representative plots of CD11c$^+$CD11b$^+$ (left) and F4/80$^+$CD11b$^+$ (middle) cells are shown; numbers indicate the percentages of differentiated cells (right).

(D) The percentage of MHCII$^+$CD80$^+$ double-positive CD11c$^+$ and F4/80$^+$ cells differentiated form spleen-derived MDSCs isolated from inflamed mice.

(E) MFI of ζ chain in normal isolated CD3$^+$ T cells coincubated for 24 hr with differentiated MDSCs (treated with GM-CSF) or poorly differentiated MDSCs (treated with BCG_{Ag}) from inflamed *Tnf*$^{+/+}$ mice at a 1:4 ratio. Before coincubation with the isolated T cells, MDSCs were cultured with GM-CSF (10 ng/ml) or BCG (50 μg/ml) for 4 days.

Results are representative of three independent experiments (error bars show SD, n = 4–5 per group). *$p < 0.02$; **$p < 0.005$ (t test). See also Figure S4.

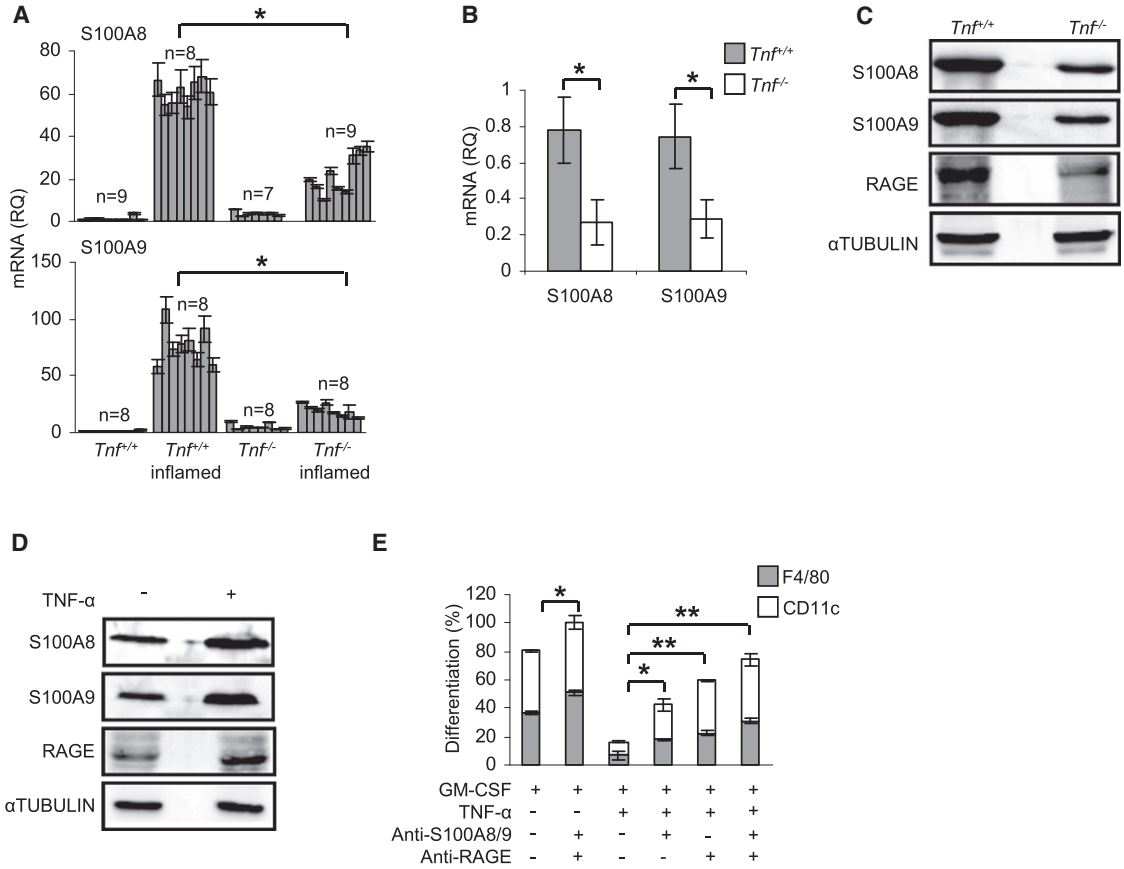

Figure 5. TNF-α Blocks MDSC Maturation via S100A8 and S100A9 and RAGE Proteins

(A) S100A8 and S100A9 mRNA expression in splenocytes are shown relative to $Tnf^{+/+}$ noninflamed mice, set as 1.

(B) S100A8 and S100A9 mRNA expression in isolated spleen-derived MDSCs is shown relative to $Tnf^{+/+}$ MDSCs (set as 1). Data of two independent experiments are presented (mean ± SEM).

(C) S100A9, S100A8, and RAGE protein expression in splenic MDSCs isolated from inflamed mice were evaluated by immunoblotting. α-Tubulin served as a control.

(D) S100A9, S100A8, and RAGE expression in splenic MDSCs isolated from inflamed $Tnf^{-/-}$ mice incubated with GM-CSF and TNF-α for 3 days were evaluated by immunoblotting. α-Tubulin served as a control.

(E) MDSCs isolated from spleens of inflamed $Tnf^{-/-}$ mice were cultured with GM-CSF, TNF-α, RAGE antibody, and S100A8 and S100A9 antibodies (together or separately) for 5 days, and cells' phenotype was evaluated. Results are representative of two or more independent experiments (error bars show SD, n = 4–9 per group).

*$p < 0.01$; **$p < 0.002$ (t test). See also Figure S5.

(Figure S6E). Taken together, these results indicate that TNF-α affects also the suppressive activity of MDSCs.

In Vivo Blockade of TNF-α under Chronic Inflammatory Conditions Modulates MDSCs and Restores Immune Functions

Our final goal was to prove the direct in vivo TNF-α role in modulating MDSC maturation and activity in $Tnf^{+/+}$ mice exhibiting chronic inflammation and to show that specific neutralization of extracellular TNF-α restores immune functions. To this end, we used the TNF-α antagonist etanercept and administrated it daily, starting 1 day before the second BCG injection, when the onset of MDSC accumulation was observed in the blood, and continuing until 1 day before the mice were sacrificed (Figure 7A). Efficacy of etanercept treatment on inflamed $Tnf^{+/+}$ mice was evaluated by comparing between their immune status and that of the inflamed $Tnf^{-/-}$ mice. Reduced spleen weight was observed in the inflamed etanercept-treated $Tnf^{+/+}$ mice compared with the etanercept-untreated inflamed $Tnf^{+/+}$ group (Figure S7A). Significant differences were also observed in the accumulation of MDSCs in the spleen: the etanercept-treated group showed a decreased percentage (Figure 7B) and total numbers (Figure S7B) of splenic MDSCs. Moreover, the reduced accumulation of MDSCs within the etanercept-treated group was accompanied by a significant increase in $CD11b^+CD11c^+$ and $CD11b^+F4/80^+$ cells within the spleen (Figures 7C and S7C), indicating an etanercept effect on MDSC maturation, similar to that observed in the inflamed $Tnf^{-/-}$ mice. Etanercept also had a significant effect on MDSC activity, as reflected by their reduced production of NO^- (Figure S7D) and ROS (Figure S7E) in the inflamed etanercept-treated group.

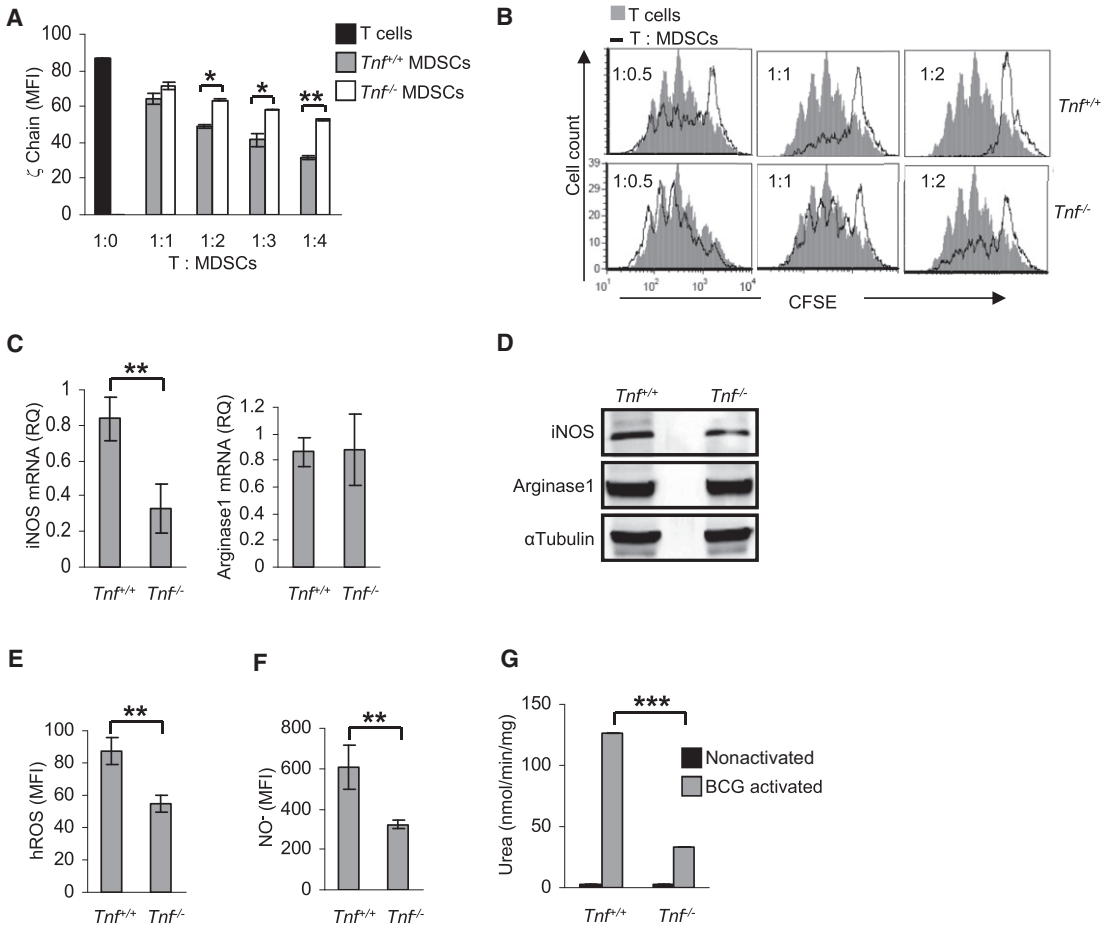

Figure 6. TNF-α Enhances MDSC Suppressive Activity

(A) Purified normal CD3$^+$ T cells were coincubated with isolated spleen-derived MDSCs from inflamed mice at different ratios. After 16 hr, ζ chain expression (MFI) in T cells was analyzed and compared to T cells incubated alone.

(B) CFSE-labeled CD3$^+$ T cells activated with CD3 and CD28 antibodies were coincubated with isolated spleen-derived MDSCs from inflamed mice at different ratios. Proliferation was assessed by monitoring cell divisions of gated CFSE-labeled Thy1.2$^+$ cells after 72 hr and compared to CD3$^+$ T cells activated alone.

(C) Analysis of iNOS and arginase 1 mRNA in isolated spleen-derived MDSCs from inflamed mice relative to the expression in *Tnf*$^{+/+}$ MDSCs (set as 1). Data of two experiments are presented (mean ± SEM).

(D) Immunoblotting of iNOS and arginase 1 in isolated spleen-derived MDSCs from inflamed mice. α-Tubulin served as a control.

(E and F) Intracellular concentration of ROS (E) and NO$^-$ (F) in spleen-derived MDSCs from inflamed mice were evaluated.

(G) Spleen-derived MDSCs isolated from inflamed mice were stimulated with BCG (50 μg/ml) for 48 hr. Cell lysates were collected and measured for arginase 1 activity. Results are representative of three independent experiments (error bars show SD, n = 4–5 per group).

*$p < 0.02$; **$p < 0.005$; ***$p < 0.0003$ (t test). See also Figure S6.

We next tested the effect of etanercept treatment on the host's immune status as well as on adoptively transferred T and NK cells. We hypothesized that etanercept treatment, by enabling MDSC maturation and reducing their suppressive activity, could rescue the response of endogenous (host) immune cells as well as of newly administered (donor) cells. To this end, CFSE-labeled normal splenocytes were administered i.v. at the peak of the inflammatory response (day +1) and were harvested after 24 hr, thus mimicking cell mediated-based therapies. Comparing ζ chain expression in donor (CFSE$^+$) and host (CFSE$^-$) T and NK cells localized in the spleen of inflamed *Tnf*$^{+/+}$ mice to those measured in control mice revealed that etanercept administration to the inflamed *Tnf*$^{+/+}$ mice significantly increased ζ chain expression in T (Figure 7D) and NK (Figure 7E) cells, both in the host and in the adoptively transferred (donor) cells. Evaluation of etanercept effects on in vivo NK and T cell function under chronic inflammatory conditions showed reconstitution of both NK cell and T cell activities. A significant elevation in the percentage of specific allogeneic cell clearance was observed in the etanercept-treated group compared to the etanercept-untreated group, both in the spleen and blood (Figure 7F). Moreover, we also found that etanercept treatment of inflamed *Tnf*$^{+/+}$ mice completely restored the ability of T cells to proliferate in vivo as observed in the normal *Tnf*$^{+/+}$ mice (Figure 7G). Taken together, these results emphasize that in vivo blockade of TNF-α leads to restoration of immune functions under chronic inflammatory conditions by modulating MDSCs.

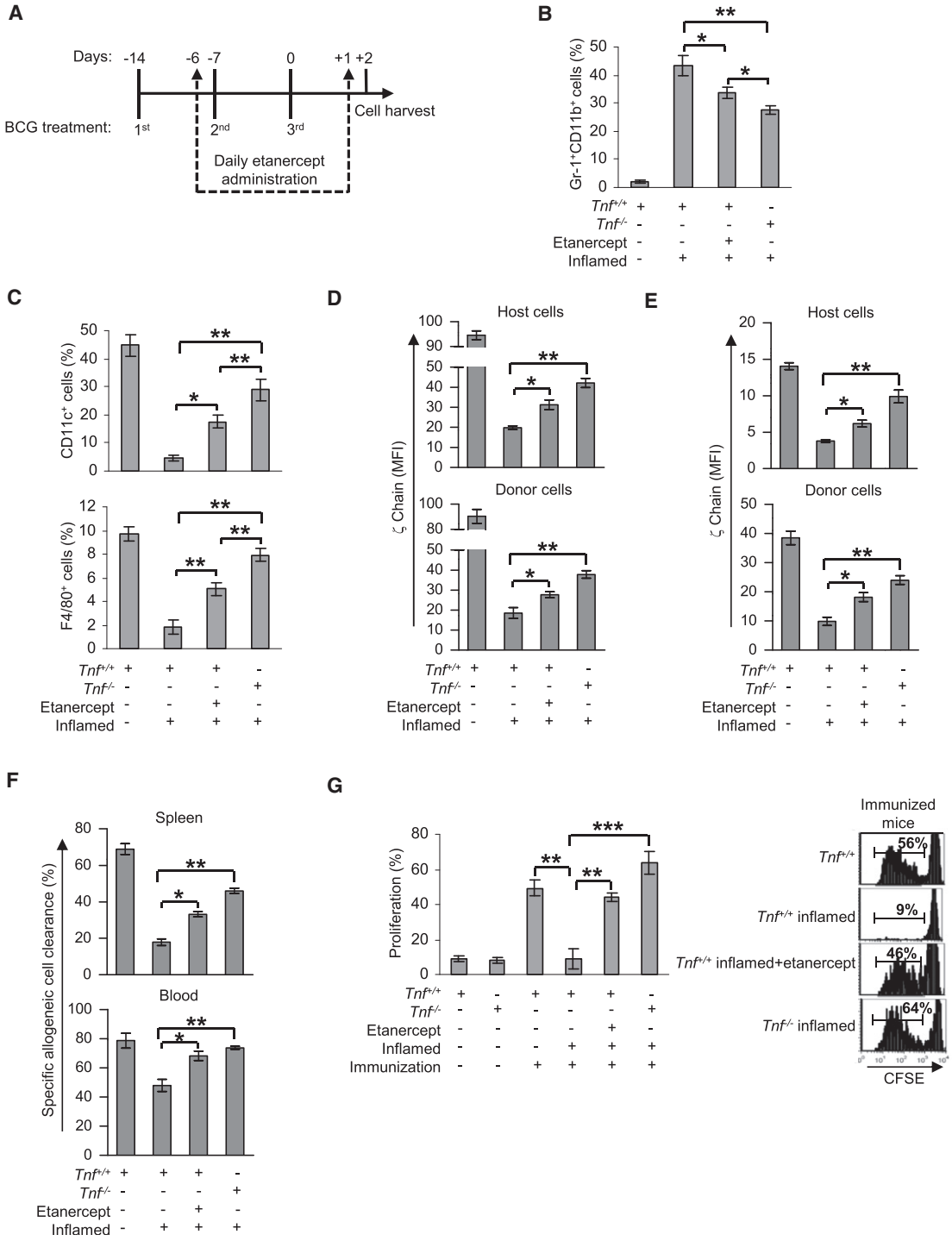

Figure 7. Administration of Etanercept Modulates MDSCs and Restores Immune Functions

(A) WT mice were injected daily with etanercept from 1 day prior to the second BCG injection until 1 day before mice were sacrificed.

(B) The percentage of MDSCs in the spleen is presented.

(C) Percentage of CD11c$^+$ and F4/80$^+$ cells in spleens is presented; plots are gated on CD11b$^+$ cells.

(D and E) CFSE-labeled splenocytes from normal *Tnf*$^{+/+}$ mice (donor cells) were adoptively transferred into mice (hosts). After 24 hr, splenocytes were harvested and stained for ζ expression (MFI) in CD3$^+$ T (D) and NCR1$^+$ NK (E) cells within the CFSE$^+$ (donor) or CFSE$^-$ (host) cells.

(F) In vivo NK cytotoxicity assay was performed as described in Figure 3D. Allogeneic cell clearance in the spleen and blood are presented.

(G) In vivo T cell proliferation was performed as described in Figure 2E. A representative plot gated on dividing OT-I CD8$^+$ T cells in the spleens (right); numbers indicate the percentage of dividing cells (left).

Results are representative of two independent experiments (error bars show SD, n = 7 per group). *p < 0.02; **p < 0.003; ***p < 0.0005 (t test). See also Figure S7.

DISCUSSION

TNF-α is a pleiotropic cytokine with both proinflammatory and immunoregulatory functions, implicated in the development of autoimmune diseases, chronic infections, and cancer, all characterized by chronic inflammation and immunosuppression (Balkwill, 2006; Feldmann, 2002; Kopf et al., 2010; Reich et al., 2005). Although TNF-α has been unequivocally validated as a therapeutic target in such immune-mediated inflammatory disorders, the mechanism by which this cytokine manipulates the host's immune system toward the generation of a suppressive environment remains unclear. A number of possible mechanisms for TNF-α-mediated immunosuppressive effects have emerged, such as inducing lymphocyte apoptosis, inhibiting TCR signaling and DC function, and activating Treg cells (Nagar et al., 2010; O'Shea et al., 2002). However, the results are in many cases complicated or controversial due to indications that both timing and duration of TNF-α expression are important in determining pathogenic versus protective roles.

Our results showing increased TNF-α concentration in the serum (Vaknin et al., 2008) and elevated gene expression in isolated MDSCs from chronically inflamed mice led us to hypothesize that TNF-α could play a role in inducing the immunosuppressive milieu observed during chronic inflammation. To test our hypothesis, we applied our previously described in vivo mouse model system for chronic inflammation, which mimics the immunosuppressive conditions generated in the above-mentioned chronic pathologies (Bronstein-Sitton et al., 2003; Vaknin et al., 2008), on *Tnf*$^{-/-}$ and *Tnf*$^{+/+}$ mice and compared their immune competence under the generated inflammatory conditions. A follow-up of these mice revealed that TNF-α plays a key role in inducing the immunosuppressive environment generated during chronic inflammation by directly affecting MDSCs in two ways: arresting their maturation and enhancing their suppressive function. These lead to an impaired immune status as reflected by T and NK cell in vivo dysfunction in association with ζ chain downregulation.

We have demonstrated that in the cell-mediated suppressive milieu generated during chronic inflammation, MDSCs are the cells primarily affected by TNF-α; although decreased MDSC numbers were significantly observed in inflamed *Tnf*$^{-/-}$ mice, Treg cell numbers remained unchanged. The lack of TNF-α also did not affect the relative distribution of the two major MDSC granulocytic and monocytic subsets (Dietlin et al., 2007; Youn et al., 2008), which were reported to differ in their function during chronic infectious diseases and cancer. However, we have demonstrated that lack of TNF-α affected MDSC maturation, as reflected by the increased accumulation of both highly mature macrophages and DCs in inflamed *Tnf*$^{-/-}$ mice, indicated by their double-positive MHC-II^{+}CD80^{+} phenotype. We also have shown that TNF-α directly affects MDSC maturation ex vivo in response to GM-CSF stimulation; inflamed *Tnf*$^{-/-}$ MDSCs display an increased ex vivo maturation capacity compared to inflamed *Tnf*$^{+/+}$ MDSCs. The enhanced MDSC maturation in the inflamed *Tnf*$^{-/-}$ mice was due to low expression of RAGE and its ligands, the S100A8 and S100A9 proteins; although the increased maturation capacity of inflamed *Tnf*$^{-/-}$ MDSCs was blocked upon incubation with exogenously added TNF-α, an almost complete restoration of MDSC differentiation was observed when using neutralizing antibodies for the RAGE receptor and the S100A8 and S100A9 proinflammatory proteins. Moreover, it was previously shown that TNF-α regulates in vitro the expression of the S100A8 and S100A9 proteins in mouse microvascular endothelial cells and macrophages (Xu and Geczy, 2000; Yen et al., 1997), as well as of the corresponding receptor, RAGE. Here we have demonstrated that indeed TNF-α regulates both the expression of RAGE and S100A8 and S100A9 mediators in MDSCs. Previous studies reported S100A8 and S100A9 as proinflammatory mediators operating in an autocrine feedback loop that sustains arrest of MDSC maturation and enhances their accumulation (Cheng et al., 2008; Sinha et al., 2008). However, these studies did not show the TNF-α effect on the expression of these proteins in MDSCs. Based on these and our observations, we suggest that during chronic inflammation, TNF-α induces increased S100A8 and S100A9 and RAGE production, which is associated with poor MDSC differentiation into mature myeloid cells, conditions that could be reversed by neutralizing TNF-α or blocking RAGE and its ligands, the S100A8 and S100A9 proteins. Additional proinflammatory cytokines such as IL-1β, IL-6, and prostaglandin E2 have been also described as mediating MDSC accumulation at tumor sites, displaying characteristics of a chronic inflammatory environment (Bunt et al., 2006, 2007; Sinha et al., 2007; Song et al., 2005). Whether these cytokines affect MDSC differentiation and S100A8 and S100A9 or RAGE expression in concert with TNF-α will necessitate further studies.

Notably, TNF-α exhibits a broader effect on MDSCs, affecting not only their maturation but also their suppressive function. A significantly reduced production of ROS and activity of both iNOS and arginase 1 was detected in MDSCs isolated from inflamed *Tnf*$^{-/-}$ mice compared to *Tnf*$^{+/+}$ mice, which was accompanied by reduced immunosuppressive activity as indicated by elevated expression of ζ chain and the pronounced in vivo and ex vivo T cell proliferation in response to activating stimuli and NK cell cytotoxic function. We also show that the impaired immune function of both T and NK cells observed during chronic inflammation was mediated by MDSCs; upon their depletion, a complete restoration of immune functions was achieved.

The direct in vivo role of TNF-α in promoting immunosuppression during a developing chronic inflammation was verified by its neutralization by etanercept injection to WT mice at the onset of the inflammatory response, where MDSC accumulation was observed in the blood, mimicking etanercept's therapeutic use. Etanercept treatment restored the host's immune function by enhancing MDSC maturation into macrophages and DCs and by abolishing their suppressive activity, resulting in the recovery of ζ chain expression and elevated T and NK cell in vivo activity. We demonstrated that the restored host's immune system features were similar between etanercept-treated inflamed *Tnf*$^{+/+}$ mice and inflamed *Tnf*$^{-/-}$ mice, strengthening our conclusion that TNF-α plays a key role in inducing an immunosuppressive environment in the course of chronic inflammation. These results obtained after etenarcept administration, which neutralized the in vivo effects of extracellular TNF-α in inflamed WT mice, and the effects observed in the ex vivo experiments where MDSCs were subjected to exogenous TNF-α show that the main role of TNF-α in the suppressive milieu is primarily mediated by its extracellular appearance. However, whether intracellular

TNF-α plays a role in modulating the suppressive cells remains an open question. Our data illuminate the mechanism underlying the beneficial effect of anti-TNF-α treatments applied in various diseases characterized by chronic inflammation and clarify the basis for the effect of etanercept treatments as shown in mice with colorectal carcinogenesis to reduce numbers of infiltrating MDSCs and lessening tumor burden (Popivanova et al., 2008).

In conclusion, the results presented here provide an insight into the relationship between TNF-α and the developing immunosuppressive environment during chronic inflammation and may aid in the generation of better therapeutic strategies against various pathologies when elevated TNF-α and MDSC amounts are detected.

EXPERIMENTAL PROCEDURES

Mice

Female C57BL/6 and BALB/c mice 6–8 weeks of age were purchased from Harlan and were grown at the Hebrew University specific-pathogen-free facility. *Tnf*-deficient mice on a C57BL/6 background were obtained from the Jackson Laboratory and the OT-I mice on a C57BL/6 background were a gift from the laboratory of A.-H. Hovav (Institute of Dental Sciences-The Hebrew University of Jerusalem, Israel). Animal use followed protocols approved by the Hebrew University-Hadassah Medical School Institutional Animal Care and Use Committee.

The In Vivo Model System for Chronic Inflammation

Heat-killed *Mycobacterium tuberculosis*-BCG (231141; Difco Laboratories) was administrated by three subcutaneous injections (50 μg per animal/dose) at 1 week intervals to induce chronic inflammation. The first two injections were administrated as a mixture of BCG and IFA (Sigma) at a 1:1 ratio, and the third BCG injection was with PBS only. Unless stated otherwise, cells were collected 2 days after the last injection (day +2). Control mice were subjected to the same protocol, but injected with PBS only.

In Vivo Depletion of MDSCs

For depletion assay, 0.3 mg of Gr1 mAb (RB6-8C5) was intraperitoneally (i.p.) administrated every 3 days into $Tnf^{+/+}$ inflamed mice.

Etanercept Treatment

The TNF-α antagonist etanercept (Wyeth, UK) was administered daily (0.5 mg/dose) by systemic i.p. injection starting from 1 day before the second BCG injection until 1 day before cell harvest. Control mice were injected with PBS.

Flow Cytometry and Antibodies

Monoclonal antibodies specific for CD16 and CD32 (93; Biolegend) were used for blockade of Fc receptors before staining. The antibodies used for cell surface labeling were FITC-labeled anti-Gr-1 (RB6-8C5; Biolegend), anti-CD11c (N418; Biolegend), anti-Ly6C (HK1.4; Biolegend), and anti-CD80 (16-10A1; BD); phycoerythrin-labeled anti-Ly6G (1A8; Biolegend), anti-F4/80 (BM8; eBioscience), anti-CD3ε (145-2C11; Biolegend), and anti-mNKp46/NCR1 (FAB2225P; R&D Systems); APC-labeled anti-CD45.1 (A20; Biolegend), biotinylated anti-CD90.2 (30-H12; Biolegend), anti-CD11b (M1/70; Biolegend), anti-MHC-II (KH74; Biolegend), and anti-CD4 (RM4-5; Biolegend); these were detected by streptavidin-Cy5 (016-170-048; Jackson Immunoresearch). Intracellular staining of ζ and CD3ε chains was performed as previously described (Bronstein-Sitton et al., 2003). For $Foxp3^+$ detection (3G3; Miltenyi Biotec), a staining buffer set (eBioscience) was used according to the manufacturer's instructions. Samples were analyzed by FACSCalibur using Cell Quest software (BD).

Immunohistochemistry

Paraffin-embedded spleen tissue sections were prepared from $Tnf^{+/+}$ and $Tnf^{-/-}$ inflamed and uninflamed mice. After antigen retrieval, sections were incubated at 4°C with primary antibodies anti-CD3 (CD3-12; AbD Serotec) and anti-Gr-1, (RB6-8C5; Biolegend). For immunohistochemical staining, universal immuno-peroxidase polymer for mouse tissues (414311F; Histofine) was used, based on a horseradish peroxidase (HRP)-labeled polymer conjugated to anti-Rat. After incubation with anti-Rat for 30 min, slide staining was completed by 3–5 min incubation with DAB+Chromogen (Lab Vision), followed by counterstaining with hematoxylin. As a control, samples were stained with each antibody and reagent individually.

CFSE Staining and Ex Vivo Proliferation Assay

Splenocytes or purified T cells (20×10^6/ml) were incubated in PBS without Ca^{2+} and Mg^{2+}, containing 5 μM CFSE (Invitrogen) for 10 min at 37°C; fetal calf serum (FCS) was then added, and the cells were washed in RPMI+8% FCS. CFSE-labeled cells were activated with 0.5 μg/ml of CD3ε (145-2C11; Biolegend) and CD28 (37.51; Biolegend) antibodies. The number of cell divisions of $Thy1.2^+$ cells was determined by flow cytometry.

In Vivo NK Cell Cytotoxicity Assay

The in vivo cytotoxic activity of NK cells was determined as previously described (Oberg et al., 2004). In brief, splenocytes from BALB/c and C57BL/6 mice were stained with CFSE (Invitrogen), at final concentrations of 0.5 μM ($CFSE^{lo}$) and 5 μM ($CFSE^{hi}$), respectively. Cells (5×10^{10}) of each type were mixed and injected into the tail vain of recipient C57BL/6 mice. PBLs and spleen cells were harvested 24 hr postinjection and the ratio between the $CFSE^{hi}$ and $CFSE^{lo}$ cells was determined based on the flow cytometry analysis. The percentage of specific allogeneic cell clearance was calculated as described before (Vaknin et al., 2008).

In Vivo T Cell Proliferation Assay

The in vivo proliferation of T cells was performed as previously described (Elnekave et al., 2010). In brief, mice were injected with 50 μg of CMV-OVA plasmid into the ear pinna by a 31-gauge needle. Seven days later, chronic inflammation was induced in some of the groups and at day +2, after the last BCG injection, $CFSE^+$ OT-I $CD45.1^+$ splenocytes were i.v. injected into the recipient $CD45.2^+$ mice. Four days after the cell transfer, mice were sacrificed and spleens were harvested. CFSE dilution were determined by flow cytometry with CD8 and CD45.1 antibodies.

Cell Isolation and Separation

MDSCs and T cells from control or inflamed mice were isolated with a magnetic column separation system (Miltenyi Biotec), as previously described (Ezernitchi et al., 2006), by performing two cycles of purifications, one with Gr1 antibodies and a second one with CD11b antibodies. The purity of cell populations was >95%.

MDSC Differentiation Assay

MDSCs were isolated from inflamed mice and cultured in the presence or absence of 10 ng/ml GM-CSF (PeproTech) for 3 and 5 days. In some experiments, 100 ng/ml of TNF-α (PeproTech) and a mixture of 10 μg/ml of RAGE (AF1179; R&D Systems) and 20 μg/ml of S100A8 and S100A9 (AF3059 and AF2065; R&D Systems) neutralizing antibodies were added to the cells, which were incubated with GM-CSF. After the different incubation periods, cell phenotypes were determined by flow cytometry analysis.

Quantitative PCR

Total RNA was recovered from splenocytes or isolated MDSCs by Tri-Reagent (Sigma) and was subjected to reverse transcription with m-MLV-RT (Invitrogen) and random primers (IDT). Quantitative mRNA expression was analyzed by real-time PCR (ABI 7900) with SYBR green (Invitrogen). RT-PCR primers are listed in Table S1 and were designed to recognize an exon-exon boundary in all transcripts.

Immunoblot Analysis

Proteins were extracted from isolated MDSCs (8×10^6) by standard techniques. The following primary antibodies were used: iNOS (54/iNOS; BD Transduction Laboratories), Arg1 (sc-18354; Santa Cruz), RAGE (AF1179; R&D Systems), S100A9 (AF2065; R&D Systems), S100A8 (AF3059; R&D Systems), and α Tubulin (sc-8035; Santa Cruz).

Arginase Activity Test

Arginase activity was measured in cell lysates from isolated MDSCs, as previously described (Corraliza et al., 1994). Urea concentration was measured at 540 nm with a microplate reader (Bio-Rad). Urea contents were calculated based on a serially diluted urea standard curve.

NO^- and ROS Measurements

iNOS activity was evaluated by measuring intracellular NO^- in $Gr1^+CD11b^+$ cells by using the DAF-2DA reagent (NOS 200-1; Cell Technology). ROS production in $Gr1^+CD11b^+$ cells was performed by reactive oxygen species detection kit (APF 4011; Cell Technology). In both cases, the detection of NO^- and ROS was performed according to the manufacturer's instructions and was determined by flow cytometry analysis after staining.

Statistical Analysis

Student's t test was used for statistical analysis. p values <0.05 were considered statistically significant.

SUPPLEMENTAL INFORMATION

Supplemental Information includes seven figures and one table and can be found with this article online at http://dx.doi.org/10.1016/j.immuni.2013.02.007.

ACKNOWLEDGMENTS

We gratefully acknowledge the support of the Society of Research Associates of the Lautenberg Center, the Concern Foundation of Los Angeles, and the Harold B. Abramson Chair in Immunology. We thank I. Vaknin for his help and advice. This study was supported by the Israel Science Foundation (ISF), the Israeli Ministry of Health, the Joint German-Israeli Research Program (DKFZ-MOST), the Israel Cancer Research Fund (ICRF), the United States-Israel Binational Science Foundation (BSF), and the Joseph and Matilda Melnick Funds.

Received: September 9, 2011
Accepted: November 13, 2012
Published: March 7, 2013

REFERENCES

Balkwill, F. (2006). TNF-alpha in promotion and progression of cancer. Cancer Metastasis Rev. *25*, 409–416.

Baniyash, M. (2004). TCR zeta-chain downregulation: curtailing an excessive inflammatory immune response. Nat. Rev. Immunol. *4*, 675–687.

Baniyash, M. (2006). Chronic inflammation, immunosuppression and cancer: new insights and outlook. Semin. Cancer Biol. *16*, 80–88.

Binder, C., Schulz, M., Hiddemann, W., and Oellerich, M. (1999). Induction of inducible nitric oxide synthase is an essential part of tumor necrosis factor-alpha-induced apoptosis in MCF-7 and other epithelial tumor cells. Lab. Invest. *79*, 1703–1712.

Bronstein-Sitton, N., Cohen-Daniel, L., Vaknin, I., Ezernitchi, A.V., Leshem, B., Halabi, A., Houri-Hadad, Y., Greenbaum, E., Zakay-Rones, Z., Shapira, L., and Baniyash, M. (2003). Sustained exposure to bacterial antigen induces interferon-gamma-dependent T cell receptor zeta down-regulation and impaired T cell function. Nat. Immunol. *4*, 957–964.

Bronte, V., and Zanovello, P. (2005). Regulation of immune responses by L-arginine metabolism. Nat. Rev. Immunol. *5*, 641–654.

Bunt, S.K., Sinha, P., Clements, V.K., Leips, J., and Ostrand-Rosenberg, S. (2006). Inflammation induces myeloid-derived suppressor cells that facilitate tumor progression. J. Immunol. *176*, 284–290.

Bunt, S.K., Yang, L., Sinha, P., Clements, V.K., Leips, J., and Ostrand-Rosenberg, S. (2007). Reduced inflammation in the tumor microenvironment delays the accumulation of myeloid-derived suppressor cells and limits tumor progression. Cancer Res. *67*, 10019–10026.

Cheng, P., Corzo, C.A., Luetteke, N., Yu, B., Nagaraj, S., Bui, M.M., Ortiz, M., Nacken, W., Sorg, C., Vogl, T., et al. (2008). Inhibition of dendritic cell differentiation and accumulation of myeloid-derived suppressor cells in cancer is regulated by S100A9 protein. J. Exp. Med. *205*, 2235–2249.

Corraliza, I.M., Campo, M.L., Soler, G., and Modolell, M. (1994). Determination of arginase activity in macrophages: a micromethod. J. Immunol. Methods *174*, 231–235.

Dietlin, T.A., Hofman, F.M., Lund, B.T., Gilmore, W., Stohlman, S.A., and van der Veen, R.C. (2007). Mycobacteria-induced Gr-1+ subsets from distinct myeloid lineages have opposite effects on T cell expansion. J. Leukoc. Biol. *81*, 1205–1212.

Elnekave, M., Furmanov, K., Nudel, I., Arizon, M., Clausen, B.E., and Hovav, A.H. (2010). Directly transfected langerin+ dermal dendritic cells potentiate CD8+ T cell responses following intradermal plasmid DNA immunization. J. Immunol. *185*, 3463–3471.

Ezernitchi, A.V., Vaknin, I., Cohen-Daniel, L., Levy, O., Manaster, E., Halabi, A., Pikarsky, E., Shapira, L., and Baniyash, M. (2006). TCR zeta down-regulation under chronic inflammation is mediated by myeloid suppressor cells differentially distributed between various lymphatic organs. J. Immunol. *177*, 4763–4772.

Feldmann, M. (2002). Development of anti-TNF therapy for rheumatoid arthritis. Nat. Rev. Immunol. *2*, 364–371.

Friedberg, J., Jacobsen, E., Neuberg, D., Kutok, J., Munoz, O., Boussiotis, V., Reynolds, H., Fisher, D., Szot, A., Van Den Abbeele, A., and Freedman, A. (2008). Targeting the follicular lymphoma microenvironment through blockade of TNFalpha with etanercept. Leuk. Lymphoma *49*, 902–909.

Gabrilovich, D.I., and Nagaraj, S. (2009). Myeloid-derived suppressor cells as regulators of the immune system. Nat. Rev. Immunol. *9*, 162–174.

Gallina, G., Dolcetti, L., Serafini, P., De Santo, C., Marigo, I., Colombo, M.P., Basso, G., Brombacher, F., Borrello, I., Zanovello, P., et al. (2006). Tumors induce a subset of inflammatory monocytes with immunosuppressive activity on CD8+ T cells. J. Clin. Invest. *116*, 2777–2790.

Gao, X., Xu, X., Belmadani, S., Park, Y., Tang, Z., Feldman, A.M., Chilian, W.M., and Zhang, C. (2007). TNF-alpha contributes to endothelial dysfunction by up-regulating arginase in ischemia/reperfusion injury. Arterioscler. Thromb. Vasc. Biol. *27*, 1269–1275.

Gebhardt, C., Németh, J., Angel, P., and Hess, J. (2006). S100A8 and S100A9 in inflammation and cancer. Biochem. Pharmacol. *72*, 1622–1631.

Goffe, B., and Cather, J.C. (2003). Etanercept: An overview. J. Am. Acad. Dermatol. *49*(2, Suppl), S105–S111.

Huang, B., Lei, Z., Zhao, J., Gong, W., Liu, J., Chen, Z., Liu, Y., Li, D., Yuan, Y., Zhang, G.M., and Feng, Z.H. (2007). CCL2/CCR2 pathway mediates recruitment of myeloid suppressor cells to cancers. Cancer Lett. *252*, 86–92.

Huye, L.E., and Dotti, G. (2010). Designing T cells for cancer immunotherapy. Discov. Med. *9*, 297–303.

Kanterman, J., Sade-Feldman, M., and Baniyash, M. (2012). New insights into chronic inflammation-induced immunosuppression. Semin. Cancer Biol. *22*, 307–318.

Kopf, M., Bachmann, M.F., and Marsland, B.J. (2010). Averting inflammation by targeting the cytokine environment. Nat. Rev. Drug Discov. *9*, 703–718.

Kusmartsev, S., Eruslanov, E., Kübler, H., Tseng, T., Sakai, Y., Su, Z., Kaliberov, S., Heiser, A., Rosser, C., Dahm, P., et al. (2008). Oxidative stress regulates expression of VEGFR1 in myeloid cells: link to tumor-induced immune suppression in renal cell carcinoma. J. Immunol. *181*, 346–353.

Mao, H., Tu, W., Liu, Y., Qin, G., Zheng, J., Chan, P.L., Lam, K.T., Peiris, J.S., and Lau, Y.L. (2010). Inhibition of human natural killer cell activity by influenza virions and hemagglutinin. J. Virol. *84*, 4148–4157.

Nagar, M., Jacob-Hirsch, J., Vernitsky, H., Berkun, Y., Ben-Horin, S., Amariglio, N., Bank, I., Kloog, Y., Rechavi, G., and Goldstein, I. (2010). TNF activates a NF-kappaB-regulated cellular program in human CD45RA- regulatory T cells that modulates their suppressive function. J. Immunol. *184*, 3570–3581.

O'Shea, J.J., Ma, A., and Lipsky, P. (2002). Cytokines and autoimmunity. Nat. Rev. Immunol. *2*, 37–45.

Oberg, L., Johansson, S., Michaëlsson, J., Tomasello, E., Vivier, E., Kärre, K., and Höglund, P. (2004). Loss or mismatch of MHC class I is sufficient to trigger NK cell-mediated rejection of resting lymphocytes in vivo - role of KARAP/DAP12-dependent and -independent pathways. Eur. J. Immunol. *34*, 1646–1653.

Ostrand-Rosenberg, S., and Sinha, P. (2009). Myeloid-derived suppressor cells: linking inflammation and cancer. J. Immunol. *182*, 4499–4506.

Pfeffer, K. (2003). Biological functions of tumor necrosis factor cytokines and their receptors. Cytokine Growth Factor Rev. *14*, 185–191.

Popivanova, B.K., Kitamura, K., Wu, Y., Kondo, T., Kagaya, T., Kaneko, S., Oshima, M., Fujii, C., and Mukaida, N. (2008). Blocking TNF-alpha in mice reduces colorectal carcinogenesis associated with chronic colitis. J. Clin. Invest. *118*, 560–570.

Reich, K., Nestle, F.O., Papp, K., Ortonne, J.P., Evans, R., Guzzo, C., Li, S., Dooley, L.T., and Griffiths, C.E.; EXPRESS study investigators. (2005). Infliximab induction and maintenance therapy for moderate-to-severe psoriasis: a phase III, multicentre, double-blind trial. Lancet *366*, 1367–1374.

Rodríguez, P.C., and Ochoa, A.C. (2008). Arginine regulation by myeloid derived suppressor cells and tolerance in cancer: mechanisms and therapeutic perspectives. Immunol. Rev. *222*, 180–191.

Scott, D.L. (2005). Etanercept in arthritis. Int. J. Clin. Pract. *59*, 114–118.

Serafini, P., Carbley, R., Noonan, K.A., Tan, G., Bronte, V., and Borrello, I. (2004). High-dose granulocyte-macrophage colony-stimulating factor-producing vaccines impair the immune response through the recruitment of myeloid suppressor cells. Cancer Res. *64*, 6337–6343.

Serafini, P., Borrello, I., and Bronte, V. (2006). Myeloid suppressor cells in cancer: recruitment, phenotype, properties, and mechanisms of immune suppression. Semin. Cancer Biol. *16*, 53–65.

Sinha, P., Clements, V.K., Fulton, A.M., and Ostrand-Rosenberg, S. (2007). Prostaglandin E2 promotes tumor progression by inducing myeloid-derived suppressor cells. Cancer Res. *67*, 4507–4513.

Sinha, P., Okoro, C., Foell, D., Freeze, H.H., Ostrand-Rosenberg, S., and Srikrishna, G. (2008). Proinflammatory S100 proteins regulate the accumulation of myeloid-derived suppressor cells. J. Immunol. *181*, 4666–4675.

Song, X., Krelin, Y., Dvorkin, T., Bjorkdahl, O., Segal, S., Dinarello, C.A., Voronov, E., and Apte, R.N. (2005). CD11b+/Gr-1+ immature myeloid cells mediate suppression of T cells in mice bearing tumors of IL-1beta-secreting cells. J. Immunol. *175*, 8200–8208.

Sutlu, T., and Alici, E. (2009). Natural killer cell-based immunotherapy in cancer: current insights and future prospects. J. Intern. Med. *266*, 154–181.

Vaknin, I., Blinder, L., Wang, L., Gazit, R., Shapira, E., Genina, O., Pines, M., Pikarsky, E., and Baniyash, M. (2008). A common pathway mediated through Toll-like receptors leads to T- and natural killer-cell immunosuppression. Blood *111*, 1437–1447.

Vignali, D.A., Collison, L.W., and Workman, C.J. (2008). How regulatory T cells work. Nat. Rev. Immunol. *8*, 523–532.

Wilson, J.A. (2008). Tumor necrosis factor alpha and colitis-associated colon cancer. N. Engl. J. Med. *358*, 2733–2734.

Xu, K., and Geczy, C.L. (2000). IFN-gamma and TNF regulate macrophage expression of the chemotactic S100 protein S100A8. J. Immunol. *164*, 4916–4923.

Yang, L., Huang, J., Ren, X., Gorska, A.E., Chytil, A., Aakre, M., Carbone, D.P., Matrisian, L.M., Richmond, A., Lin, P.C., and Moses, H.L. (2008). Abrogation of TGF beta signaling in mammary carcinomas recruits Gr-1+CD11b+ myeloid cells that promote metastasis. Cancer Cell *13*, 23–35.

Yen, T., Harrison, C.A., Devery, J.M., Leong, S., Iismaa, S.E., Yoshimura, T., and Geczy, C.L. (1997). Induction of the S100 chemotactic protein, CP-10, in murine microvascular endothelial cells by proinflammatory stimuli. Blood *90*, 4812–4821.

Youn, J.I., Nagaraj, S., Collazo, M., and Gabrilovich, D.I. (2008). Subsets of myeloid-derived suppressor cells in tumor-bearing mice. J. Immunol. *181*, 5791–5802.